Supplemental Information

A super stable assembled P nanowire with variant structural and magnetic/electronic properties via transition metal adsorption

Shukai Wang,[a,#] Jinxing Gu,[b,#] Yinan Dong,[a] Linwei Sai,[c] Fengyu Li,[a,*]

[a] *School of Physical Science and Technology, Inner Mongolia University, Hohhot, 010021, China*

[b] *Department of Chemistry, The Institute for Functional Nanomaterials, University of Puerto Rico, Rio Piedras Campus, San Juan, PR 00931, USA*

[c] *College of Science, Hohai University, Changzhou 213022, China*

* Corresponding Author: fengyuli@imu.edu.cn (FL); zhaojj@dlut.edu.cn (JZ)
[#] Equal contributions

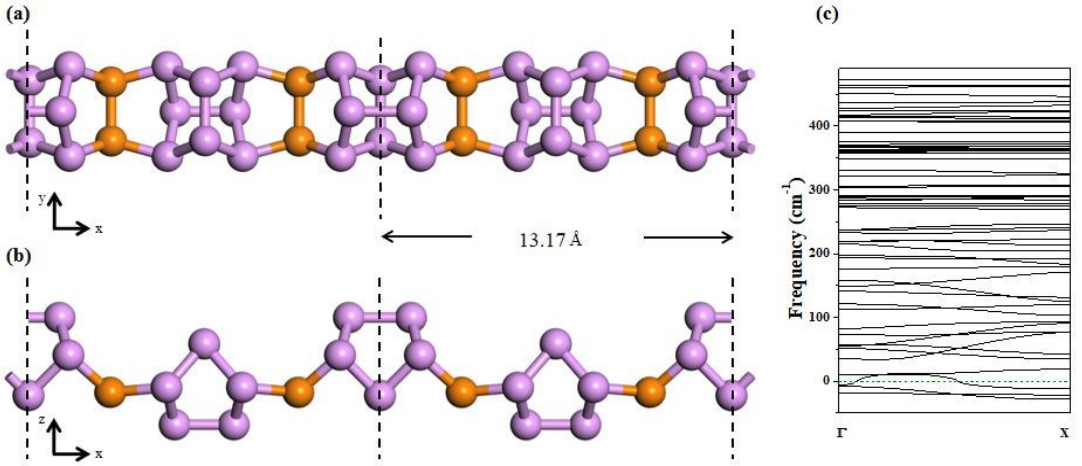

Fig. S1 Two views (a,b) and the calculated phonon spectrum (c) of the 1D-P_{20} NW. The unitcell was marked by black dashed lines. The P_2 dimers are in orange.

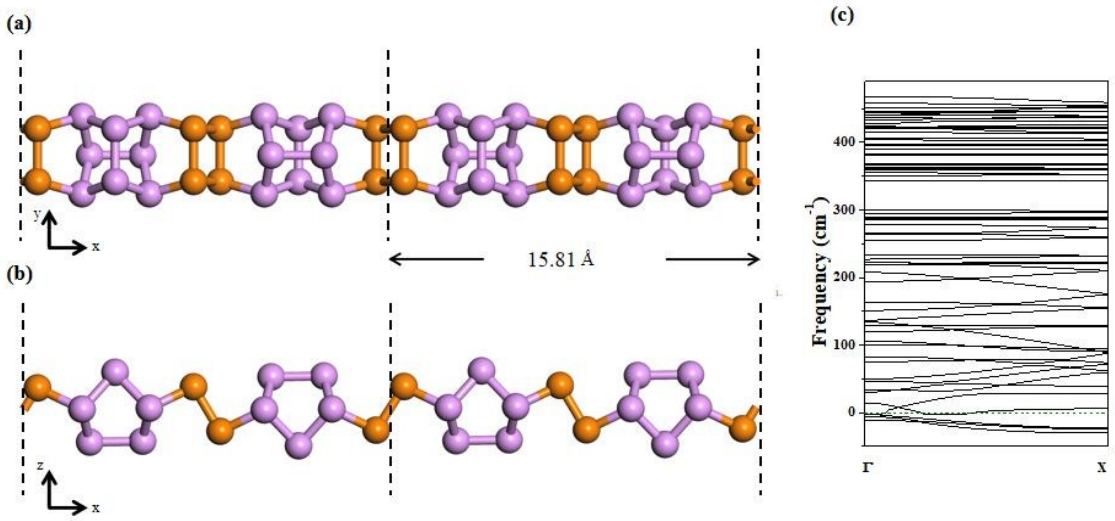

Fig. S2 Two views (a,b) and the calculated phonon spectrum (c) of the 1D-P_{24} NW. The unitcell was marked by black dashed lines. The P_2 dimers are in orange.

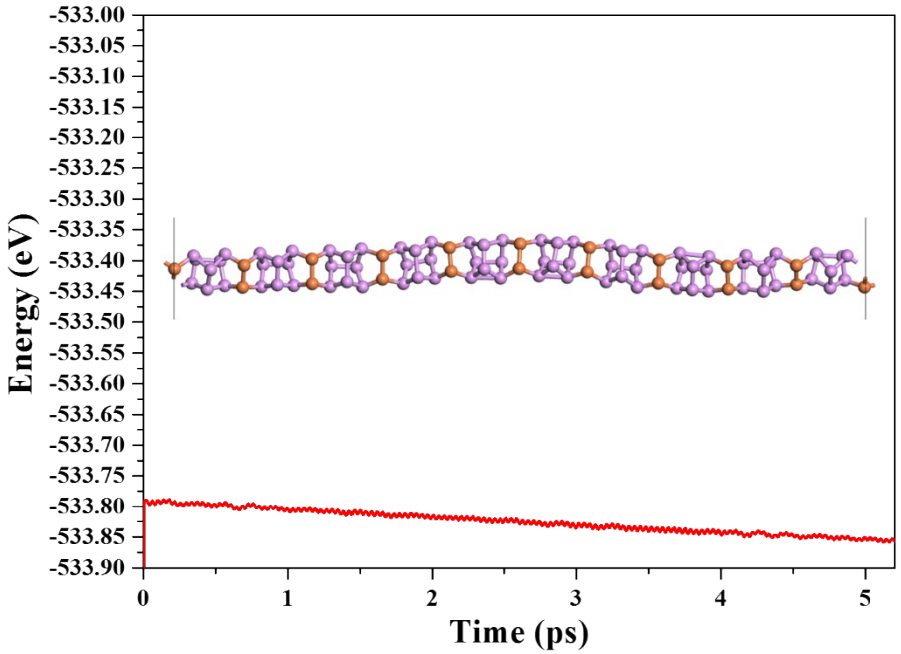

Fig. S3 The evolution of total energies of the 1D-P_{10} NW (a 10×1×1 supercell, 100 P atoms in total) and the structural snapshot of the MD simulation at 300 K for at the end of 5.2 ps. The P_2 dimers are in orange.

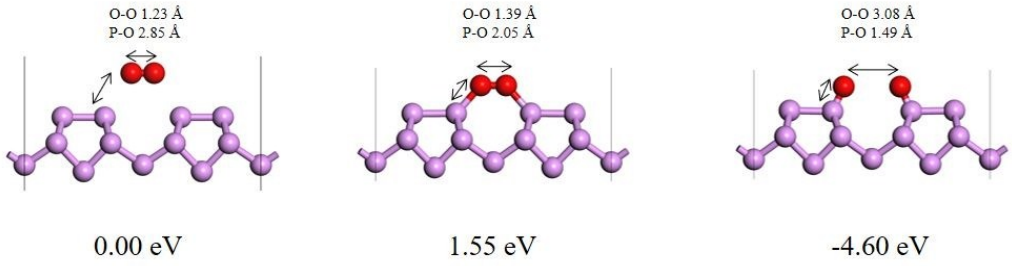

Fig. S4 The adsorption and dissociation behaviors of the 1D-P_{10} NW regarding to O_2 molecules, as well as the changes in bond length.

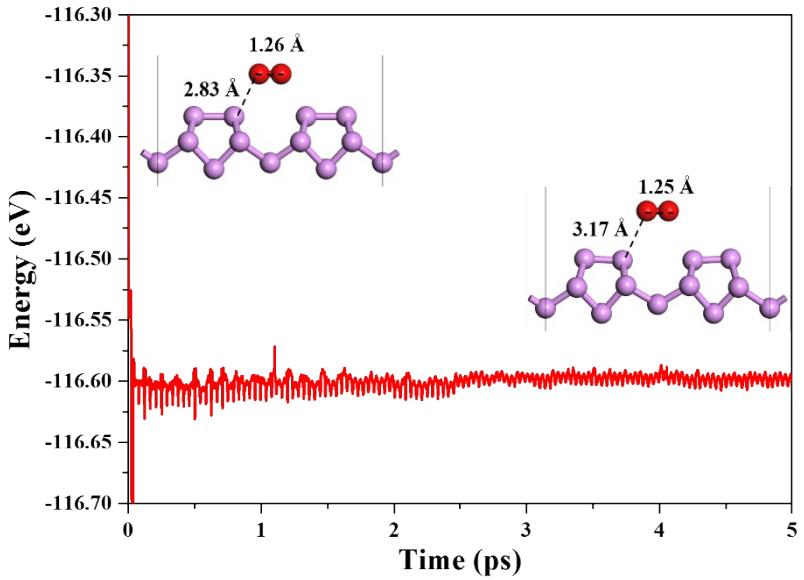

Fig. S5 The evolution of total energies of the 1D-P_{10} NW (a 2×1×1 supercell) with one O_2 molecule and the structural snapshot of the MD simulation at 500 K for at the end of 5 ps.

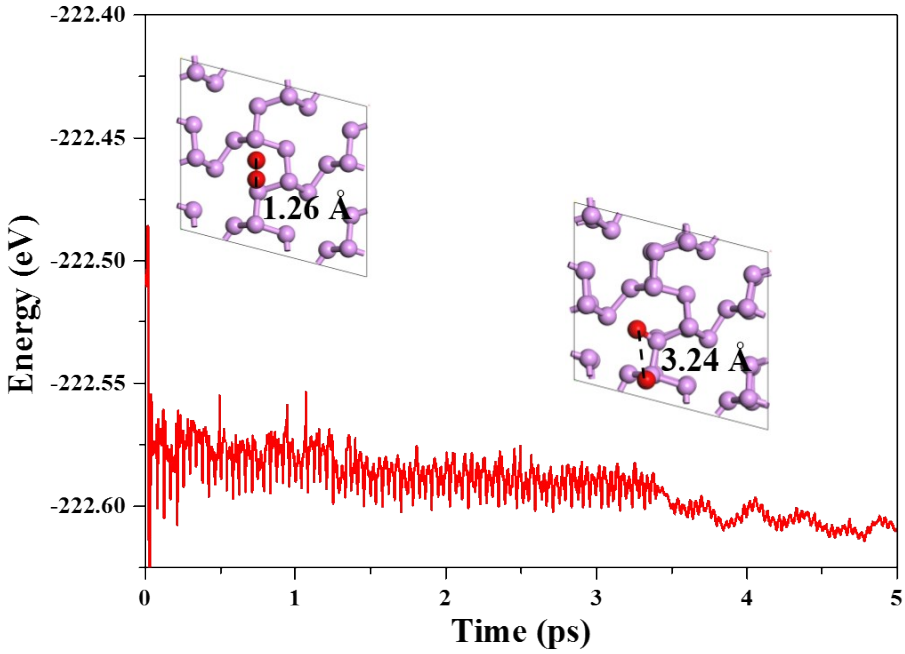

Fig. S6 The evolution of total energies of the 2D θ-P (a 2×2×1 supercell) with one O_2 molecule and the structural snapshot of the MD simulation at 300 K for at the end of 5 ps.

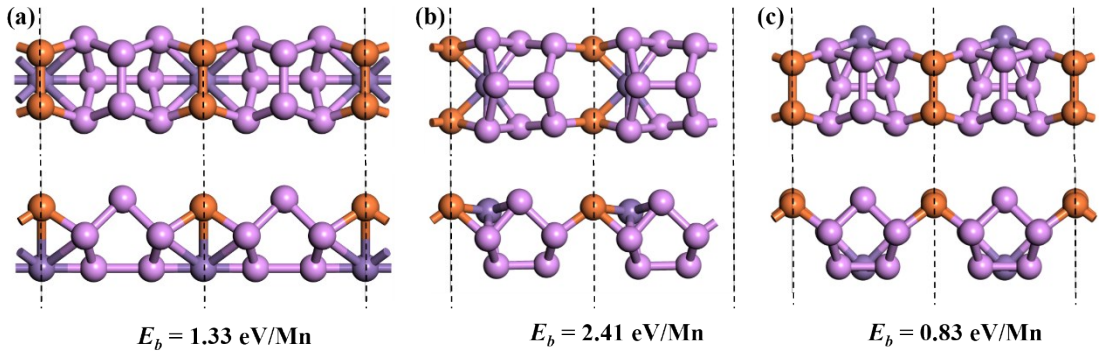

Fig. S7 Two views of the three optimized structures of Mn_1@1D-P_{10}: Mn_1-A (a), Mn_1-B (b), Mn_1-C (c). The P_2 dimers are in orange.

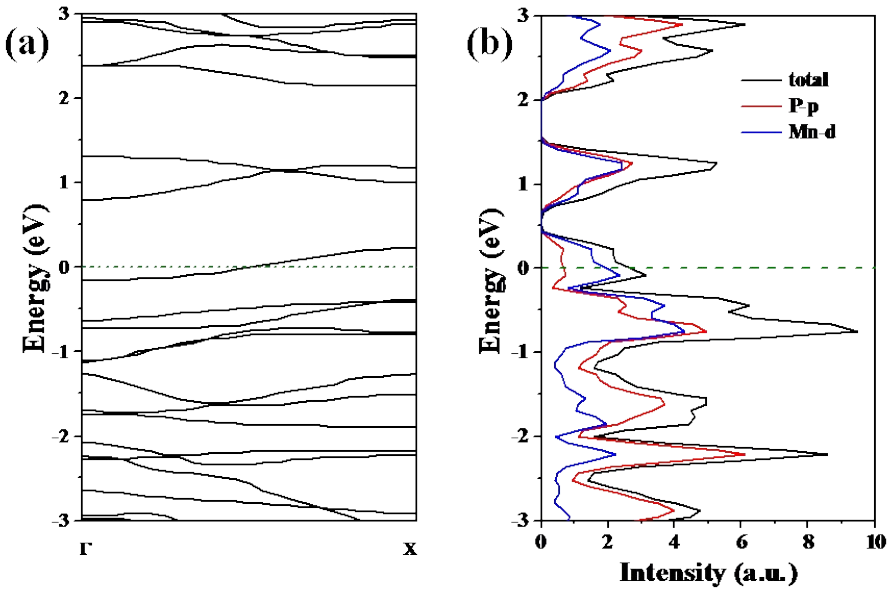

Fig. S8 The PBE+U band structure (a) and density of states (b) of the 1D-Mn_1@P_{10} with Mn adsorbed at the Mn_1-B site.

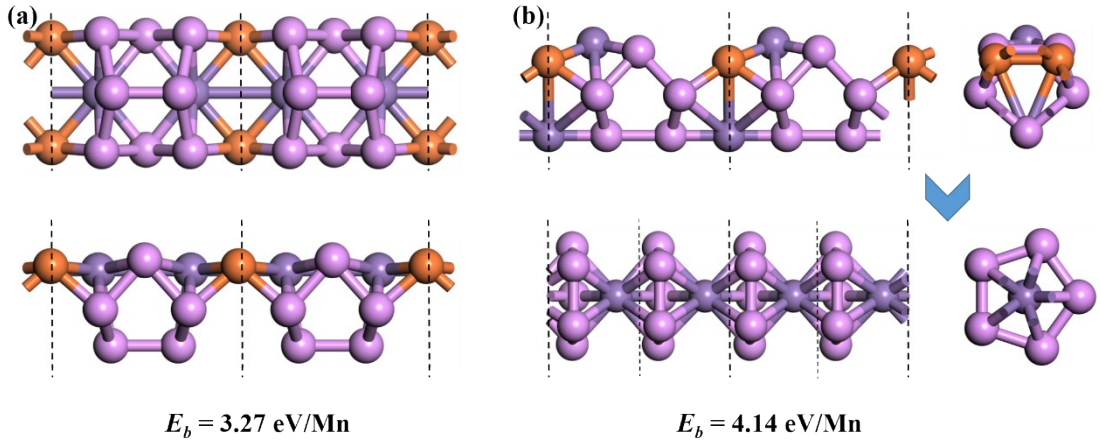

Fig. S9 Two views of the two optimized structures of Mn_2@1D-P_{10}: Mn_2-BB (a), Mn_2-BA (b). The P_2 dimers are in orange.

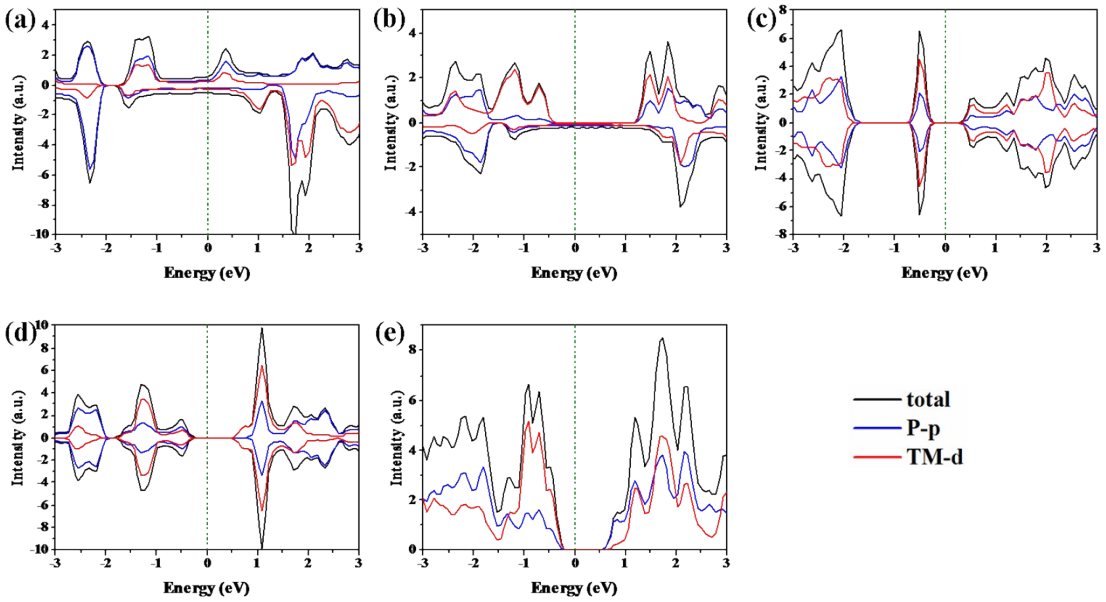

Fig. S10 The density of states of sandwich 1D-Mn_2@P_{10} (a), 1D-V_1@P_5 (b), 1D-Cr_2@P_{10} (c), 1D-Fe_2@P_{10} (d), and 1D-Mo_2@P_{10} (e) NWs. The Fermi level is set at 0 eV.

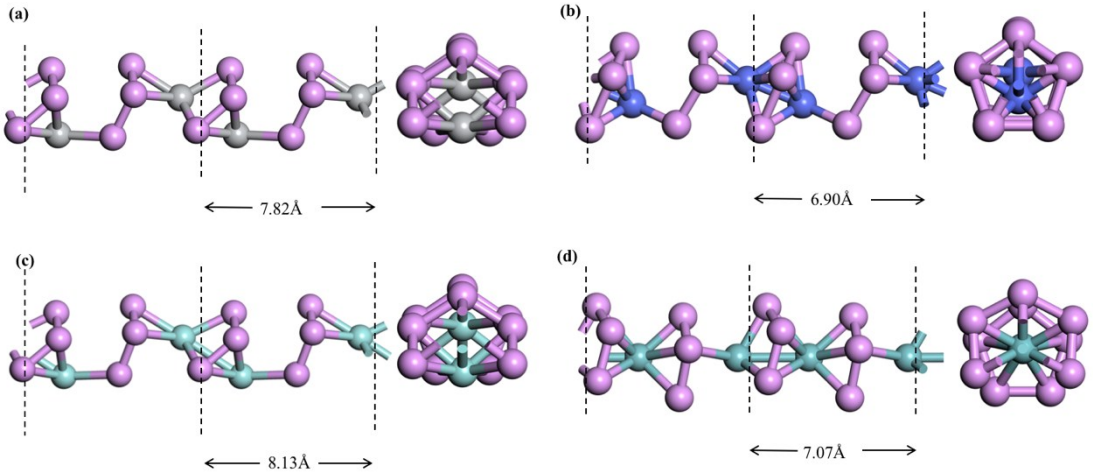

Fig. S11 Two views of the optimized structures of 1D-Ti_2@P_{10} (a), 1D-Co_2@P_{10} (b), 1D-Zr_2@P_{10} (c), and 1D-Nb_2@P_{10} (d).

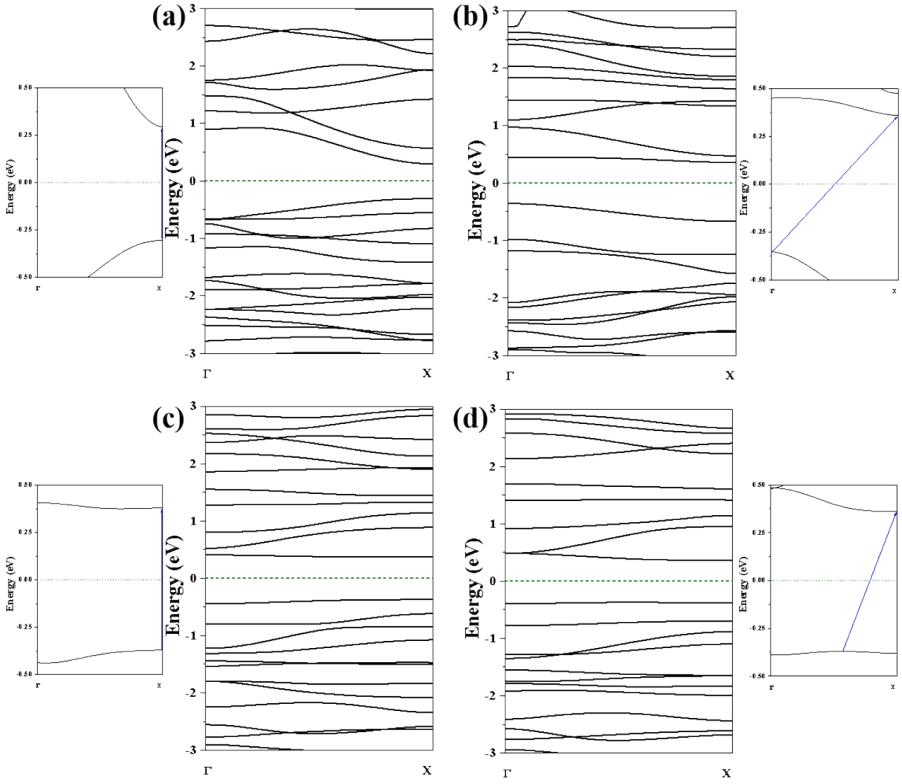

Fig. S12 The PBE+U band structures of quasi-sandwich chains 1D-Co_2@P_{10} (a), 1D-Nb_2@P_{10} (b), 1D-Ti_2@P_{10} (c), and 1D-Zr_2@P_{10} (d) NWs. The Fermi level is set at 0 eV. The zoomed insects indicate the direct-bandgap feature in the 1D-Co_2@P_{10} and 1D-Ti_2@P_{10}, and indirect-bandgap character in the 1D-Nb_2@P_{10} and 1D-Zr_2@P_{10} NWs, respectively.

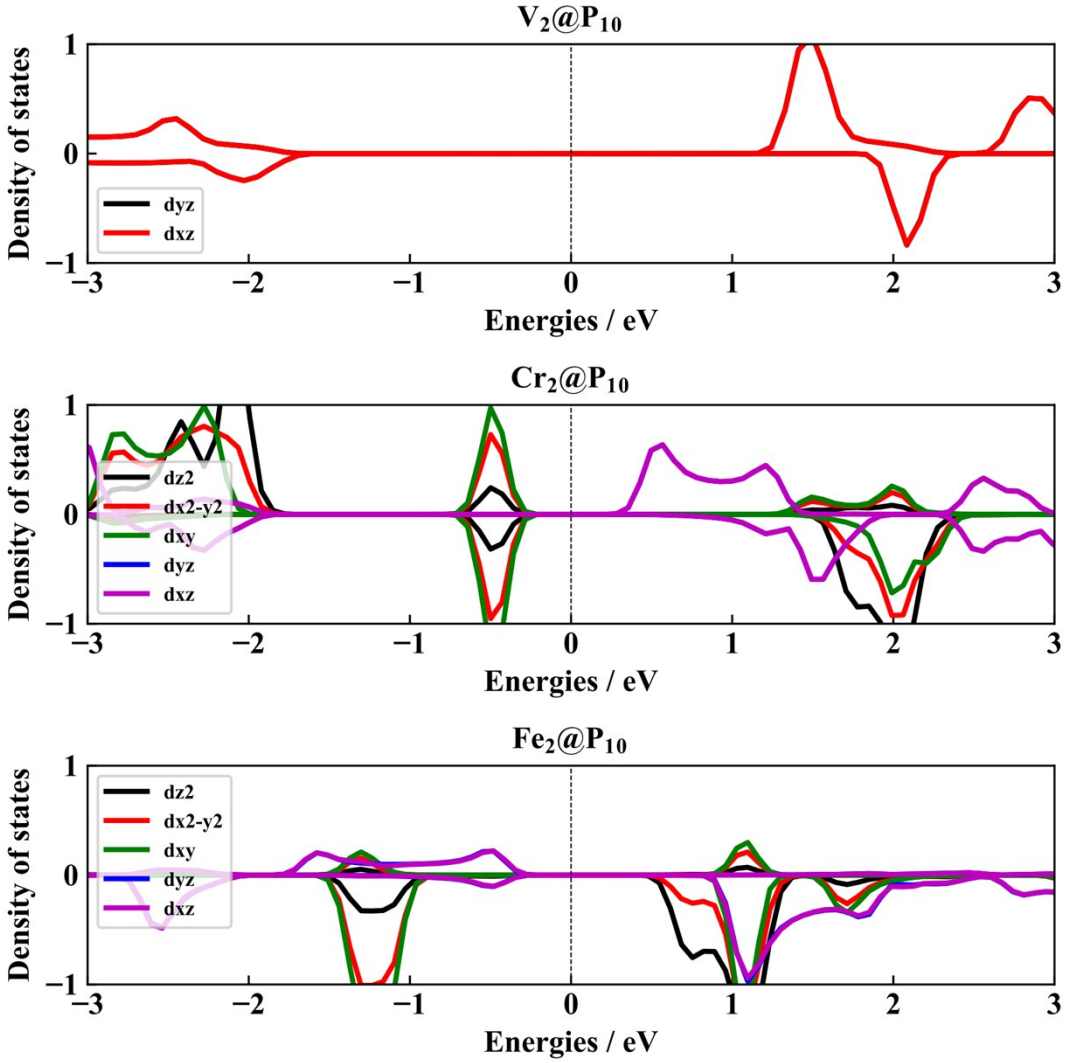

Fig. S13 The local density of states for orbital d_{xz} and d_{yz} of $V@P_5$ clearly show that the two orbitals are degenerated. For $Cr_2@P_{10}$ and $Fe_2@P_{10}$, lines representing orbital d_{xz} and d_{yz} are also overlapped, while lines for d_{xy} and d_{x2-y2} orbitals are not exactly overlapped, because these orbitals have complex interactions with P_5 rings due to their low energies.

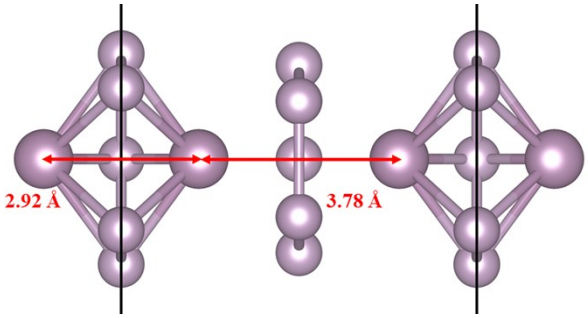

Fig. S14 The illustration of Mo…Mo separations in the $Mo_2@P_{10}$ nanowire.

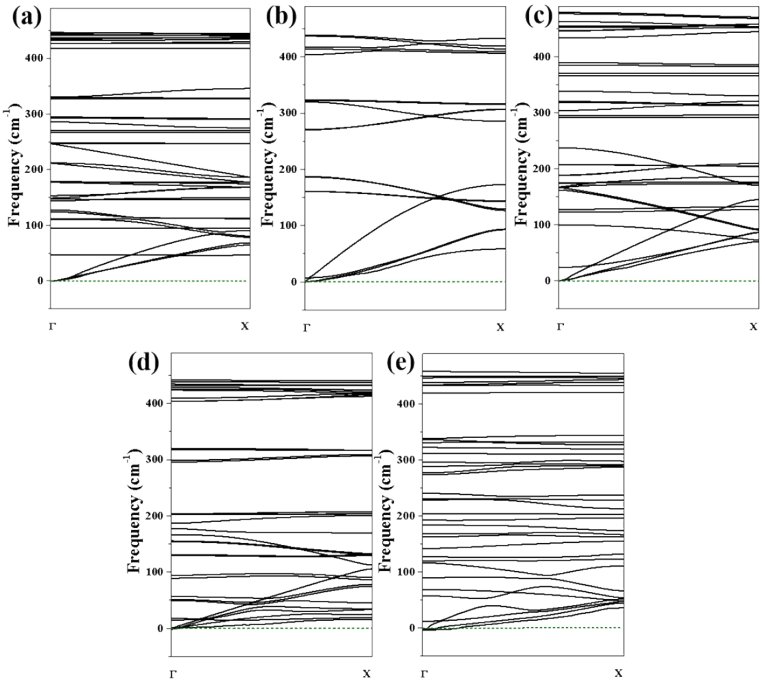

Fig. S15 The calculated phonon spectra of the sandwich chains 1D-$Mn_2@P_{10}$ (a), 1D-$V_1@P_5$ (b), 1D-$Cr_2@P_{10}$ (c), 1D-$Fe_2@P_{10}$ (d), and 1D-$Mo_2@P_{10}$ (e).

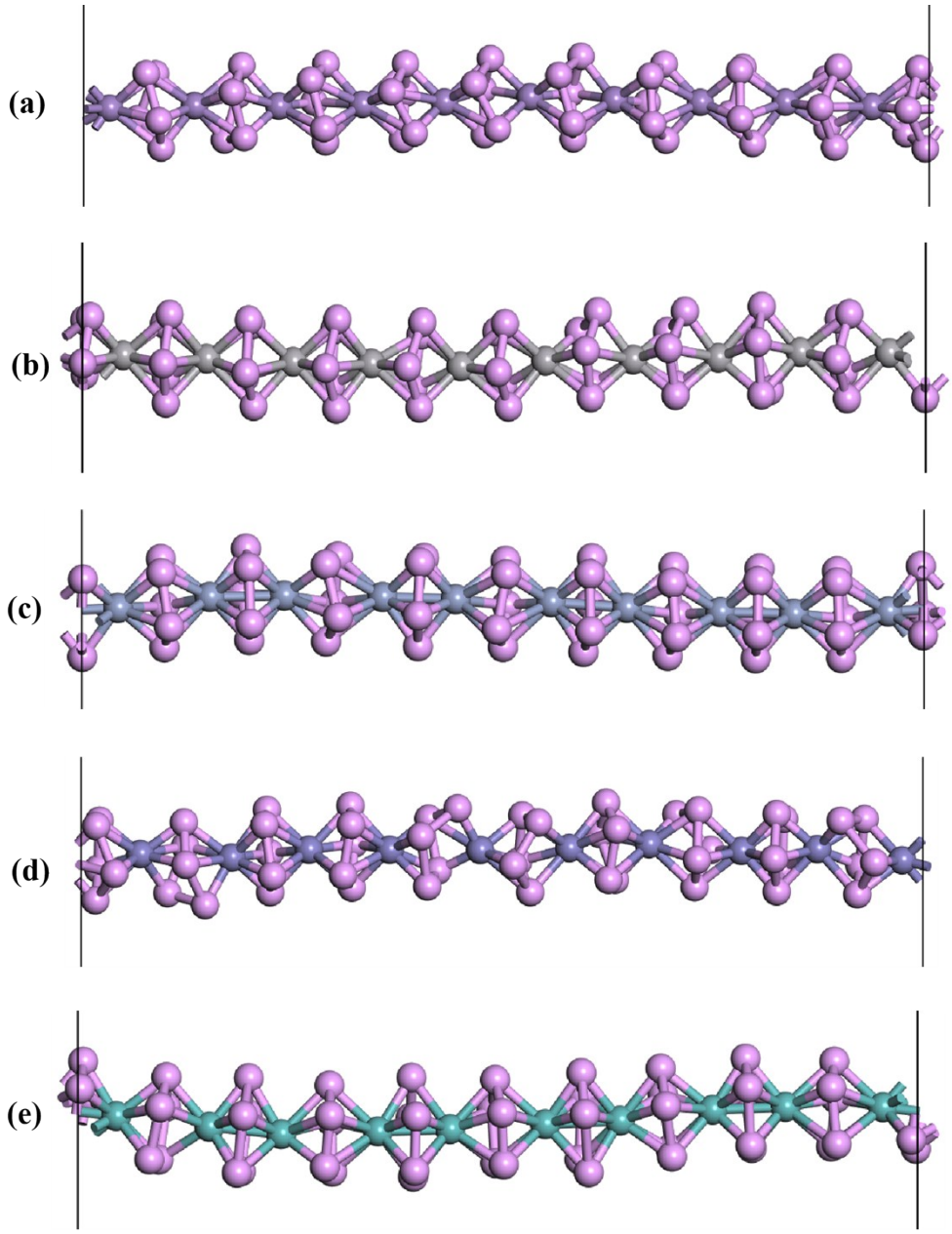

Fig. S16 The final structures of 1D $TM_2@P_{10}$ chains through a 5 ps MD simulation at room temperature (T = 300 K): (a) TM = Mn, (b) TM = V, (c) TM = Cr, (d) TM = Fe, (e) TM = Mo.

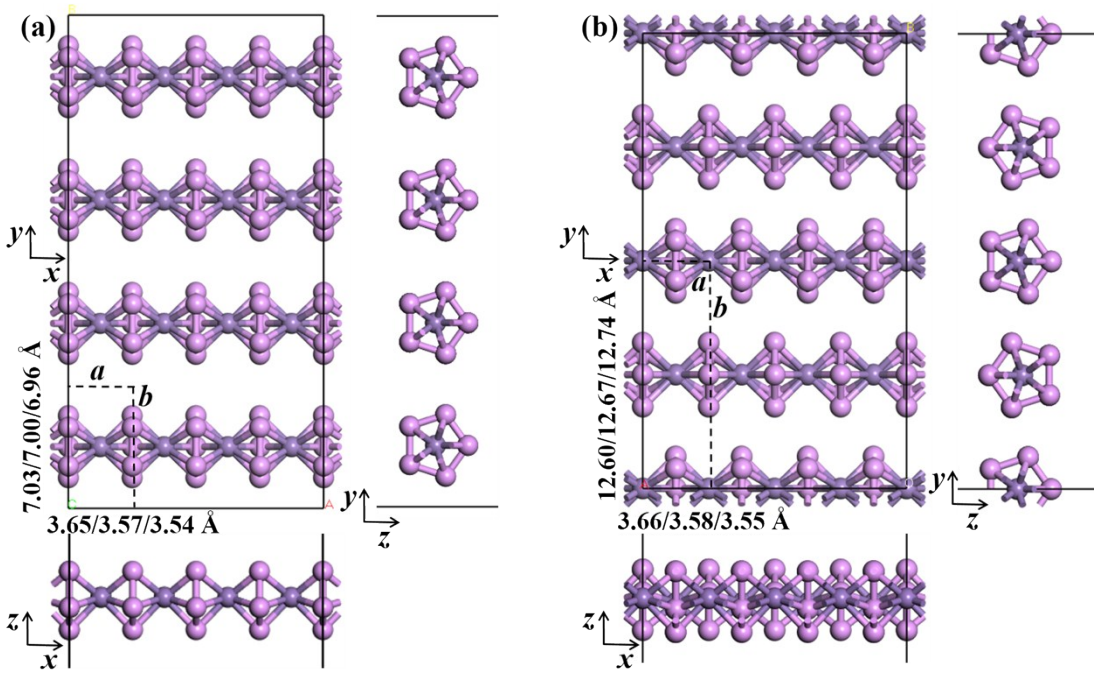

Fig. S17 The top and two side views of the vdW-type 2D sheets in (a) Type-I ($TM_1@P_5$) and (b) Type-II ($TM_2@P_{10}$) configurations, TM = Mn/V/Cr.

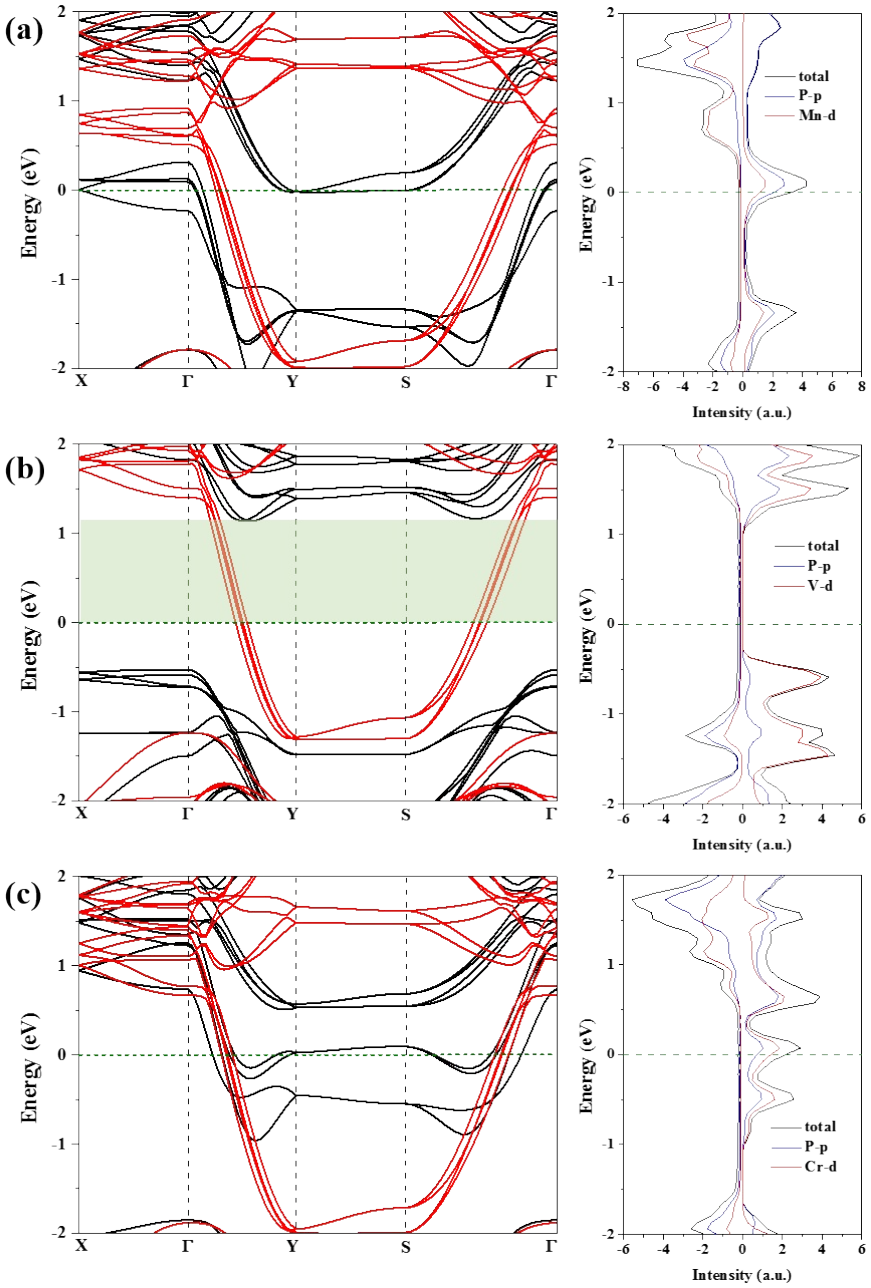

Fig. S18 The band structures (left) and density of states (right) of the vdW-type 2D sheets in Type-II ($TM_2@P_{10}$) configuration (a) TM = Mn, (b) TM = V, (c) TM = Cr.

Table S1. The relative energies (ΔE, in eV) between FM and AFM states of the sandwich 1D-$TM_2@P_{10}$ (TM = Mn, V, Cr, Fe, Mo) chains.

	Mn	V	Cr	Fe	Mo
FM	0.00	0.00	0.00	0.00	0.00
AFM	0.77	0.77	-0.30	-0.28	0.00

Table S2. The magnetic anisotropy energy (*MAE*, in meV/TM atom) and the easy axis (EA) for the sandwich 1D-$Mn_2@P_{10}$ and 1D-$V_1@P_5$ chains. The 1D NWs is along *x* axis, the 2D systems are in the *xy* plane.

	E(001)−E(100)	E(010)−E(100)	E(011)−E(100)	E(101)−E(100)	E(110)−E(100)	E(111)−E(100)	EA
1D-$Mn_2@P_{10}$	0.001	0.292	0.207	0.289	0.133	0.276	(100)
	E(001)−E(100)	E(010)−E(100)	E(011)−E(100)	E(101)−E(100)	E(110)−E(100)	E(111)−E(100)	EA
1D-$V_1@P_5$	0.010	0.291	0.154	0.086	0.286	0.027	(100)
	E(001)−E(101)	E(010)−E(101)	E(100)−E(101)	E(011)−E(101)	E(110)−E(101)	E(111)−E(101)	EA
2D-$Mn_2@P_{10}$	0.383	0.243	0.385	0.194	0.282	0.370	(101)
	E(001)−E(100)	E(010)−E(100)	E(011)−E(100)	E(101)−E(100)	E(110)−E(100)	E(111)−E(100)	EA
2D-$V_2@P_{10}$	0.002	0.314	0.166	0.317	0.085	0.004	(100)
	E(001)−E(101)	E(010)−E(101)	E(100)−E(101)	E(011)−E(101)	E(110)−E(101)	E(111)−E(101)	EA
2D-$Cr_2@P_{10}$	0.358	0.005	0.119	0.122	0.210	0.127	(101)

Table S3. The calculated number of electrons in each d suborbital for one Cr ion in the $Cr_2@P_{10}$ sandwich chain.

Orbitals	**Up electron**	**Down electron**
d_{xy}	0.78	0.30
d_{x2-y2}	0.82	0.23
d_{xz}	0.43	0.26
d_{yz}	0.43	0.26
d_{z2}	0.88	0.11